

IMPURITY CENTERS

Photosensitive Bismuth Ions in Lead Tungstate

V. A. Vazhenin^{a,*}, A. P. Potapov^a, G. R. Asatryan^{b,**}, and M. Nikl^c

^a Institute of Physics and Applied Mathematics, Ural Federal University named after the First President of Russia B.N. Yeltsin
pr. Lenina 51, Yekaterinburg, 620000 Russia

* e-mail: Vladimir.vazhenin@usu.ru

^b Ioffe Physical-Technical Institute, Russian Academy of Sciences,
Politekhnicheskaya ul. 26, St. Petersburg, 194021 Russia

** e-mail: hike.asatryan@mail.ioffe.ru

^c Institute of Physics, Czech Academy of Science,
Na Slovance 1999/2, Prague 8, 182 21 Czech Republic

Received July 6, 2012

Abstract—Electron paramagnetic resonance (EPR) signals of Bi²⁺ ions have been detected in the EPR spectrum of manganese-, bismuth-, and tin-doped PbWO₄ single-crystals irradiated by xenon and mercury lamps at 100 K. The parameters of the Zeeman, hyperfine, and superhyperfine interactions and the localization of Bi²⁺ ions have been determined.

DOI: 10.1134/S1063783413040343

1. INTRODUCTION

Lead tungstate PbWO₄ (PWO) crystals have been known as fast scintillators successfully implemented in modern high-energy physics (see [1–4] and references therein). These crystals were optimized for calorimetric detectors by doping with trivalent ions [5, 6]. Great progress in the enhancement of quantum yield was achieved by double doping of PWO crystals with Mo and La or Y and Nb ions [7–10]. This doping enhances the quantum yield by a factor of 2–4 without significant loss of other scintillation characteristics.

According to [11], internal luminescence and scintillation in PbWO₄ are of excitonic nature and the charge-transfer band in the (WO₄)²⁻ complex leads to emission in the blue part of the spectrum. Autolocalized excitons decay already at 150 K [12]. Accordingly, all shallow-trap levels in the PWO lattice at room temperature participate in trapping and become very important. They change the migration characteristics of free charge carriers by secondary trapping, in which all uncontrolled impurities and defects can have a significant effect. Successful implementation of the crystal in the above-mentioned applications requires deeper insight into the mechanisms of luminescence and, consequently, the knowledge of the structure of defects and uncontrolled impurities, which induce the specific features of charge carrier trapping in PbWO₄.

One of the most direct methods of studying the structure of impurity centers is electron paramagnetic resonance [13]. The EPR technique provides determination of the spin and charge state of the impurity, the local symmetry of the center, the structure of the nearest environment, and the specificity of interaction

with the crystal lattice. The results of the magnetic resonance studies of Nd³⁺, Ce³⁺, Gd³⁺, Mn²⁺, Fe³⁺, Cr³⁺, and other paramagnetic defects in PbWO₄ can be found elsewhere [14–17].

This work is focused on studying the EPR of new paramagnetic centers, Bi²⁺ ions, discovered in PbWO₄ for the first time.

2. EXPERIMENTAL TECHNIQUE

The measurements were carried out on a Bruker EMX Plus X-band EPR spectrometer in the temperature range of 100–170 K. We used for measurements the lead tungstate crystals (space group $I4_1/a(C_{4h}^6)$) studied in the previous works of one of us [18, 19]; in addition to manganese, the crystals were weakly doped with tin and bismuth during the growth.

The samples were irradiated by a 35-W xenon lamp or an HPML-125 mercury lamp through a special optical window in the microwave cavity of the spectrometer.

3. RESULTS AND DISCUSSION

In a wide temperature range (4–300 K), the crystals under investigation feature the intense EPR spectrum of a Mn²⁺ center thoroughly studied in the previous work of one of us [19]. This spectrum is due to the manganese ions substituting Pb²⁺ ions in the position with the local symmetry S_4 surrounded by two embedded oxygen tetrahedra, one of which is elongated and the other is compressed along the tetrahedral axis. In

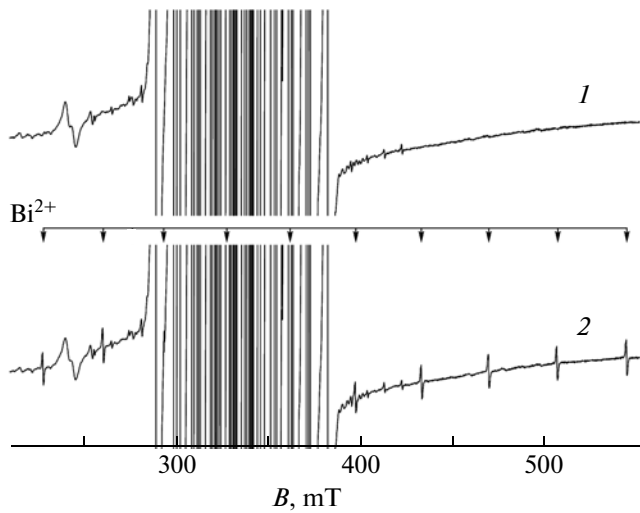


Fig. 1. Fragment of the EPR spectrum of $\text{PbWO}_4 : \text{Mn}$ at 110 K (1) before and (2) after irradiation. The intense signals seen in the center are due to a tetragonal Mn^{2+} center. Deviation of the magnetic field \mathbf{B} from the orientation $\mathbf{B} \parallel \mathbf{S}_4$ is less than 0.5° . The arrows indicate the positions of 10 hyperfine components of Bi^{2+} .

addition to the tetrahedral Mn^{2+} center, very weak signals are observed at $T \approx 100$ K, which can be assigned to transitions of triclinic centers of manganese and iron.

The irradiation of the $\text{PbWO}_4 : \text{Mn}$ samples by the xenon or mercury lamp at a temperature of ~ 100 K leads to the emergence of a new EPR spectrum shown in Fig. 1. The spectrum is dominated by the contribution from the tetragonal Mn^{2+} center, whose peak intensity is more than three orders of magnitude greater than that of the new spectrum. The observed 10-component spectrum is obviously due to the hyperfine interaction of the paramagnetic center with its own nuclear spin $9/2$. The intensity of the new spectrum increases for 10 min under irradiation. A considerable decrease in the spectrum intensity occurs under the sample heating up to 170 K. Other changes in the spectrum under irradiation and an increase in temperature were not observed.

Orientation behavior of the positions of the hyperfine components is shown in Fig. 2. Also shown are the calculated angular dependences found from the axial spin Hamiltonian (the electron spin $S = 1/2$, the nuclear spin $I = 9/2$, $\mathbf{z} \parallel \mathbf{S}_4$)

$$H_{\text{sp}} = g_{\parallel} \beta B_z S_z + g_{\perp} \beta (B_x S_x + B_y S_y) + A_{\parallel} S_z I_z + A_{\perp} (S_x I_x + S_y I_y), \quad (1)$$

where g is the electron g factor; β is the Bohr magneton; B_x , B_y , and B_z are the magnetic field components; A is the hyperfine constant; and S_x , S_y , S_z , I_x , I_y , and I_z are the operators of the components of the electron

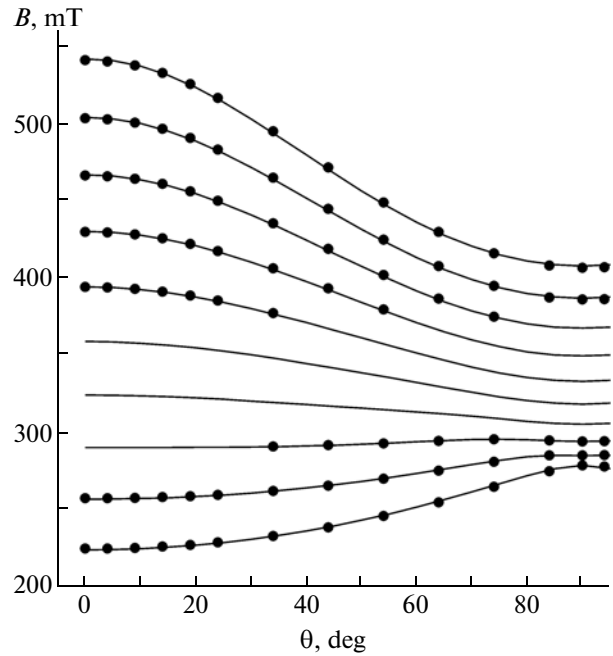


Fig. 2. Dependences of the position of the transitions in the EPR spectrum of Bi^{2+} at a frequency of 9423 MHz on the orientation in the ac plane at 110 K. Circles are the experimental points, and solid lines are the calculated angular dependences.

and nuclear spins. The parameters of the spin Hamiltonian found by fitting the experimental frequencies to the calculated ones (minimizing the root-mean-square deviation) at $\mathbf{z} \parallel \mathbf{S}_4$ are as follows:

$$\begin{aligned} g_{\parallel} &= 1.740(2), \quad |A_{\parallel}| = 857(6) \text{ MHz} \\ &\quad (\text{or } 35.2 \text{ mT}), \\ g_{\perp} &= 1.923(2), \quad |A_{\perp}| = 382(4) \text{ MHz} \\ &\quad (\text{or } 14.2 \text{ mT}). \end{aligned} \quad (2)$$

The root-mean-square deviation of 85 experimental resonance frequencies is 15 MHz. We did not observe the effect of the nuclear Zeeman and quadrupole interactions on the orientation behavior of the spectrum.

Bi^{3+} ions (state $6s^2$) introduced into the crystal in the eightfold environment have the ionic radius $R_i = 1.17 \text{ \AA}$ and most probably substitute Pb^{2+} ions ($R_i = 1.29 \text{ \AA}$). If the radiation-generated electrons are trapped by the bismuth ions, there can appear Bi^{2+} ions in the crystal. It should be mentioned that Murphy et al. [20] studied monoclinic $^{209}\text{Bi}^{2+}$ centers (ground state $6p^1$, $I = 9/2$, natural abundance 100%) in CdWO_4 crystals. Importantly, the parameters of the spin Hamiltonian found in [20] ($g_a = 1.38$, $A_a = 31.5 \text{ mT}$, $g_b = 1.543$, $A_b = 35.0 \text{ mT}$, $g_c = 1.623$, and $A_c = 28.8 \text{ mT}$; a , b , and c are the crystallographic axes

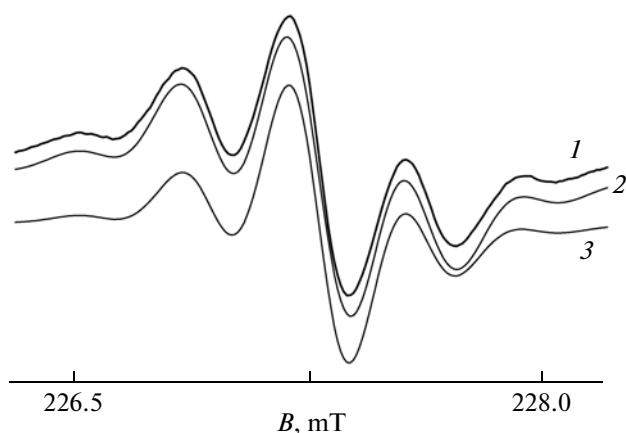


Fig. 3. Superhyperfine structure of the low-field component of the EPR spectrum of Bi^{2+} ions in $\mathbf{B} \parallel \mathbf{S}_4$ at 110 K: (1) experiment and (2, 3) simulation taking into account interaction with four equivalent lead and tungsten nuclei, respectively.

of CdWO_4) agree fairly well with parameters (2). The presence of paramagnetic niobium and indium ions with $I = 9/2$ and high abundance in PbWO_4 is quite improbable. Owing to these facts, we conclude that the spectrum merging under irradiation belongs to Bi^{2+} ions in the position of Pb^{2+} . Substitution of the W^{6+} ion with $R_i = 0.42 \text{ \AA}$ and the same symmetry \mathbf{S}_4 is ultimately improbable.

All hyperfine components of the spectrum of Bi^{2+} have superhyperfine structure (Fig. 3) that weakly depends on the nuclear spin projection. The formation of this structure is due to the interaction with either ^{207}Pb nuclei ($I = 1/2$, natural abundance 22.1%) from the nearest lead tetrahedron ($R = 4.055 \text{ \AA}$, the polar angle of the magnetic field in the crystallographic reference frame $\theta = 42.2^\circ$) or ^{183}W nuclei ($I = 1/2$, natural abundance 14.3%), forming a tungsten square with $\theta = 90^\circ$ and $R = 3.852 \text{ \AA}$. As is seen in Fig. 3, the simulation of the superhyperfine structure for $\mathbf{B} \parallel \mathbf{S}_4$ taking into account the natural abundance of the isotopes shows a much better agreement with the experiment for superhyperfine interaction with the ^{207}Pb nuclei (an effective interaction parameter of $\sim 0.68 \text{ mT}$).

The experimental superhyperfine structure of the low-field hyperfine component of the spectrum of Bi^{2+} at $\theta = 42^\circ$ and 90° , $\varphi = 0^\circ$ (φ is the azimuthal angle of the magnetic field in the crystallographic reference frame) is shown in Figs. 4 and 5 along with the results of numerical simulation of this structure. Assuming that the axis of the $\text{Bi}^{2+}-^{207}\text{Pb}$ bond forms an angle of $\sim 42^\circ$ with \mathbf{S}_4 and that the electron–nuclear interaction is axial in the local reference frame (\mathbf{z}_{loc} is parallel to the axis of the $\text{Bi}^{2+}-^{207}\text{Pb}$ bond) and neglecting the anisotropy of the g factor [21] we find

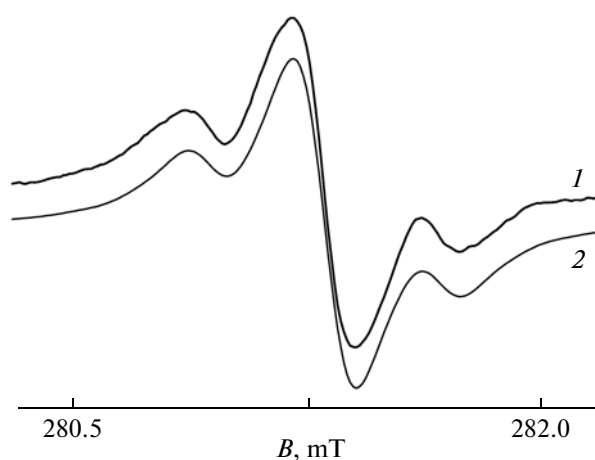


Fig. 4. (1) Experimental and (2) simulated superhyperfine structures of the low-field component of the EPR spectrum of Bi^{2+} ions in $\mathbf{B} \perp \mathbf{S}_4$ at 110 K.

the following parameters of the superhyperfine interaction:

$$|a_{\parallel}| = 0.93(7) \text{ mT}, \quad |a_{\perp}| = 0.35(5) \text{ mT}. \quad (3)$$

Naturally, it was assumed in the simulation of the spectrum that four lead nuclei are equivalent at $\mathbf{B} \parallel \mathbf{S}_4$ ($\theta_{\text{loc}} \approx 42^\circ$), there two pairs of equivalent nuclei at $\theta = 90^\circ$ ($\theta_{\text{loc}} \approx 48^\circ$ and $\approx 90^\circ$) and at $\theta = 42^\circ$, $\theta_{\text{loc}} \approx 0^\circ$ for one nucleus, $\theta_{\text{loc}} \approx 84^\circ$ for the second nucleus, and $\theta_{\text{loc}} \approx 123^\circ$ for two other nuclei. We used the line shape, which is intermediate between the Gaussian and Lorentzian with a width of $0.20\text{--}0.25 \text{ mT}$.

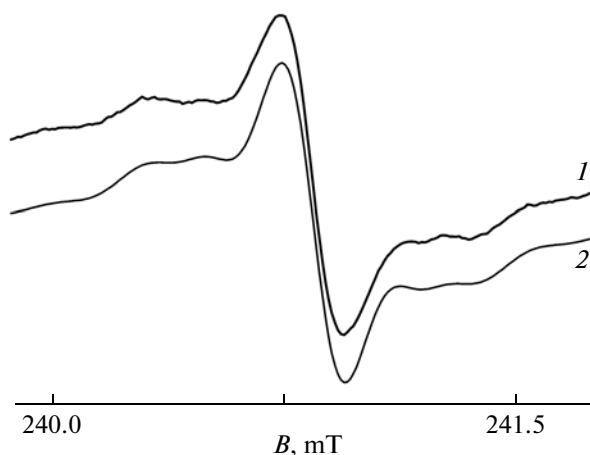


Fig. 5. (1) Experimental and (2) simulated superhyperfine structures of the low-field component of the EPR spectrum of Bi^{2+} ions in the magnetic field oriented along the bond ($\theta = 42^\circ$, $\varphi = 0$) at 110 K.

4. CONCLUSIONS

Irradiation of manganese-, bismuth-, and tin-doped PbWO_4 single crystals by a 35-W xenon lamp and an HPML-125 mercury lamp at a temperature of less than 170 K leads to the appearance of a new paramagnetic center. Based on the experimental data on the Zeeman, hyperfine, and superhyperfine interactions of the emerging center, it can be stated unambiguously that it is due to Bi^{2+} ions. The bismuth ions substituting Pb^{2+} ions in the PbWO_4 lattice interact considerably with the nearest lead ions.

ACKNOWLEDGMENTS

This study was supported by the Ministry of Education and Science of the Russian Federation (state contracts nos. 14.740.11.0048 and 16.513.12.3007) and the Russian Academy of Sciences within the framework of the programs “Spin Phenomena and Solid-State Nanostructures and Spintronics” and “Basic Foundations of Technologies of Nanostructures and Nanomaterials.”

REFERENCES

1. V. G. Baryshevski, M. Korzhik, V. I. Moroz, V. B. Pavlenko, A. F. Lobko, A. A. Fedorov, V. A. Kachanov, V. L. Solovjanov, B. I. Zadneprovsky, V. A. Nefyodov, P. V. Nefyodov, B. A. Dorogovin, and L. L. Nagornaja, *Nucl. Instrum. Methods Phys. Res., Sect. A* **322**, 231 (1992).
2. M. Kobayashi, M. Ishii, Y. Usuki, and H. Yahagi, *Nucl. Instrum. Methods Phys. Res., Sect. A* **333**, 429 (1993).
3. M. Nikl, *Phys. Status Solidi A* **178**, 595 (2000).
4. A. A. Annenkov, M. V. Korzhik, and P. Lecoq, *Nucl. Instrum. Methods Phys. Res., Sect. A* **490**, 30 (2002).
5. R. W. Novotny, D. Bremer, V. Dormenev, P. Drexler, T. Eissner, T. Kuske, and M. Moritz, *J. Phys.: Conf. Ser.* **293**, 012003 (2011).
6. S. Burachas, M. Ippolitov, V. Manko, S. Nikulin, A. Vasiliev, A. Apanasenko, A. Vasiliev, A. Uzunian, and G. Tamulaitis, *Radiat. Meas.* **45**, 83 (2010).
7. M. Nikl, P. Bohacek, A. Vedda, M. Martini, G. P. Pazzi, P. Fabeni, and M. Kobayashi, *Phys. Status Solidi A* **182**, R3 (2000).
8. A. A. Annenkov, A. E. Borisevich, A. Hofstaetter, M. V. Korzhik, P. Lecoq, V. D. Ligun, O. V. Misevitch, R. Novotny, and J. P. Peigneux, *Nucl. Instrum. Methods Phys. Res., Sect. A* **450**, 71 (2000).
9. M. Nikl, P. Bohacek, E. Mihokova, N. Solovieva, A. Vedda, M. Martini, G. P. Pazzi, P. Fabeni, and M. Kobayashi, *J. Appl. Phys.* **91**, 2791 (2002).
10. M. Nikl, P. Bohacek, E. Mihokova, N. Solovieva, A. Vedda, M. Martini, G. P. Pazzi, P. Fabeni, and M. Ishii, *J. Appl. Phys.* **91**, 5041 (2002).
11. M. J. J. Lammers, G. Blasse, and D. S. Robertson, *Phys. Status Solidi A* **63**, 569 (1981).
12. V. Murk, M. Nikl, E. Mihokova, and K. Nitsch, *J. Phys.: Condens. Matter* **9**, 249 (1997).
13. S. A. Al'tshuler and B. M. Kozyrev, *Electron Paramagnetic Resonance* (Academic, New York, 1964; Nauka, Moscow, 1972), p. 121.
14. J. Rosa, H. R. Asatryan, and M. Nikl, *Phys. Status Solidi B* **158**, 573 (1996).
15. S. V. Nistor, M. Stefan, E. Goovaerts, M. Nikl, and P. Bohacek, *J. Phys.: Condens. Matter* **18**, 719 (2006).
16. H. Yeom and A. R. Lim, *J. Korean Phys. Soc.* **49**, S562 (2006).
17. V. V. Laguta, M. Martini, A. Vedda, E. Rosetta, M. Nikl, E. Mihokova, J. Rosa, and Y. Usuki, *Phys. Rev. B: Condens. Matter* **67**, 205102 (2003).
18. S. V. Nistor, M. Stefan, E. Goovaerts, M. Nikl, and P. Bohacek, *Radiat. Meas.* **38**, 655 (2004).
19. M. Stefan, S. V. Nistor, E. Goovaerts, M. Nikl, and P. Bohacek, *J. Phys.: Condens. Matter* **17**, 719 (2005).
20. H. J. Murphy, K. T. Stevens, N. Y. Garces, M. Moldovan, N. C. Giles, and L. E. Halliburton, *Radiat. Eff. Defects Solids* **149**, 273 (1999).
21. A. Abragam and B. Bleaney, *Electron Paramagnetic Resonance of Transitions Ions* (Clarendon, Oxford, 1982; Mir, Moscow, 1972), Vol. 1, p. 217.

Translated by A. Safonov